Colgate Academic Review

Volume 8 (Fall 2010) Article 10

7-20-2012

Biomineral Structure and Strength of Barnacle Exoskeletons

Nathan B. Swift

Nathan B. Swift '11

Biomineral Structure and Strength of Barnacle Exoskeletons

Abstract

The process of building organic-inorganic compound structures through biomineralization is extremely impressive and potentially very useful. During biomineral formation, organisms restructure simple, naturally occurring minerals in conjunction with their own organically produced minerals to create new structures, the functions of which often include protection or storage, among others. While there is extensive knowledge about materials properties and structure of the raw minerals themselves, insight into how specific biomineral structures and compounds contribute to an object's mechanical properties is lacking. In this study, the exoskeletons of several barnacles from the genus Balanus were examined thoroughly, both for their physical structure (how they're put together) and for their mechanical properties (tensile strength, hardness, and elasticity). Barnacles were chosen because of their abundance in salt-water environments; their early appearance in the fossil record; and their impact on the early studies of evolution. Scanning electron microscopy produced close-up, detailed images of the inner shell structure to determine what type of structure barnacles build during exoskeleton formation. In addition, energy dispersive x-ray spectroscopy was used to map the elemental components of the shells. Nanoindentation tested the mechanical properties of these mapped structures to determine how certain characteristics of the exoskeleton contribute to its hardness, strength, and elasticity.

Introduction

The ability of mineral-producing organisms to design and create structures for their own use with utmost complexity, precision, and strength from very simple materials is a phenomenon of great mystery. Through this process called biomineralization, naturally occurring elements (Ca+, Mg2+, CO3-) are formed into a range of material structures [1]. With the help of certain essential organic components, biomineralization is a process that revolutionizes the concept of engineering by building materials from the nanoscale up, and it is a process entirely designed by nature. Yet, before we are able to harness such a practice, there is still much to learn about the formation mechanism. Our research examines the microstructure of the, calcium carbonate shells of Balanus amphitrite barnacles in an attempt to unlock the mystery behind the exoskeleton structure, its mechanical advantages, and the biomineralization process behind the exoskeleton formation.

Biomineralization

Biomineralization is the process through which organisms take naturally occurring elements and form them into complex minerals. These biologically formed minerals are often composites of both inorganic and organic materials and can vary in shape, size, crystallinity, isotopic and trace element compositions [2], unlike their geologic counterparts. One common way of structuring these two vital components is by layering the mineral crystals and organic materials [2]—much like bricks and mortar. However, there are numerous other possible structures, including many with unusual morphologies,

most of which occur at a level of complexity unattainable by human engineering.

There are two distinct processes for biomineral formation (also called nucleation [3]): biologically induced nucleation and biologically controlled nucleation [2]. The former is a process commonly used by many bacteria and fungi species [4], in which only the commencement of the biomineralization process is controlled by the organism. The rest of the process, such as type and habit of minerals used, structure, etc. is not in the direct control of the organism. Biologically induced biomineralization also occurs in the open environment, rather than a space delineated for the purpose of the process, and consequently the formed biomineral characteristically reflects the environment in which it is formed [4]. In biologically controlled biomineralization, the organism maintains control of the biomineralization characteristics throughout the procedure. The cellular activities plus enzymes and proteins from the organism fully direct the nucleation, growth, morphology, and final location of the deposited mineral, and this all occurs in an isolated environment, specifically outlined by the organism for use of biomineral construction [2], [4]. Many larger organisms, including barnacles, use this biologically controlled process in their biomineral construction.

Barnacles use calcium carbonate to form their exoskeletons, which is true of most invertebrates, whereas most biomineralizing vertebrates use calcium phosphate [3]. While calcium carbonate exists in a variety of different polymorphs (including dolomite, aragonite, calcite, and vaterite), the only calcium carbonate minerals observed thus far in barnacles are calcite and aragonite [5]-[11]. Most invertebrate biominerals nucleate from an amorphous calcium carbonate precursor (ACC), which is unstable and isotropic; therefore, ACC often goes through a phase transition into one of the other, more stable forms of calcium carbonate during biomineral formation. ACC is much harder to detect, as it does not diffract X-rays or electrons; hence, as of now, there is no solid evidence that barnacle shells actually form from this precursor [3]. However, it is strongly suspected due to ACC's abundance in other biominerals.

The primary advantage (and mystery) of biomineralization is that it can take one simple mineral and engineer it with the use of essential organic components into a wide array of structural designs, each with different functions and properties [12]. In barnacles, the shell layering and microcrystalline structure are believed to be the source of the shell's strength and resistance to erosion. One example of such mechanical advantage is found in the calcium carbonate shell produced by abalone, a marine gastropod. The abalone shell consists of an outer calcite layer and an inner aragonite layer. The inner layer, called nacre or mother-of-pearl, is formed in a distinct brick-and-mortar structure, 5% of which is organic molecules, with the other 95% consisting of inorganic aragonite tablets around 400 nanometers thick [13]. The extraordinary property of nacre is that it has 3000 times the tensile strength of the aragonite mineral from which it is formed, due in part to its extremely well ordered microstructure [14], [15]. This mechanical strength is superior to most other artificial composite ceramics, and even more natural tissues such as animal bone [16]. In 2008, Pérez-Huerta et al. [12] conducted further experiments on the calcitic "nacre" of brachiopod shells using nanoindentation to examine its mechanical properties. The study found the semi-nacre is significantly harder and stiffer than calcite fibers. The semi-nacre had a hardness of approximately 3-5 GPa and elasticity of 50-85 GPa, whereas the calcite fibers only had a hardness of 0.4-3 GPa and elasticity 30-60 GPa.

Barnacle Structure

Barnacles are crustacean arthropods, meaning that they are closely related to other marine creatures such as crabs, lobsters, and shrimp [17]. Arthropods carry similar traits, such as nutrition via filter-feeding and a hard outer shell. However, unlike its crustacean cousins, the barnacle is a sessile creature [17], meaning that it spends the majority of its life in one place, attached to a hard substrate, such as a rock or a boat. The short time in the organism's life when it actually is mobile occurs during the first of two life stages, which lasts for roughly the first 10-45 days in the barnacle's life, when it is a swimming larva [17] looking for a substrate onto which it will attach itself for the remainder of its adult life. The immobility of the adult stage makes it impossible for barnacles to use one of the major defense mechanisms against predators—the ability to run away. To compensate for this increased vulnerability, barnacles have a second calcareous (calcium carbonate-based) outer shell called the test or exoskeleton, in addition to the standard chitin-based crustacean shell [1], [17], giving the creature a far stronger layer of physical protection, as can be seen in Figure 1 (see appendix).

It is this exoskeleton that is the focus of this research. The exoskeleton of barnacles from the genus Balanus is two-layered, matrixed together with embedded secondary structures of oriented crystals, which are usually in the shape of prisms [18]. It has two major mineralogical and chemical components: calcium carbonate and organic matter, the latter of which constitutes just above 1% of the shell's mass [18]-[20]. Specifically, data shows B. amphitrite has about 4.7% organic material by mass, whereas B. eburnesus only contains about 1.6%, which is far less than that observed in nacre [13], [21]. Clare et al. (1994) [22] report that in growth, the exoskeleton of B. amphitrite builds in increments, leaving characteristic layers that are visible as lateral rows in exoskeleton cross-section SEM images. On the macroscopic level, the shell is made up of separate plates, which when layered together form the semi-circular exoskeleton encasing the organism's body. These layered plate connections are evident in Figure 2 (see appendix). Above the organism's body is an additional two-plate shell called the operculum, which is not directly attached to the outer shell, but rather, to the top of the body of the animal, providing protection from the open mantle cavity [22]. The organism is able to open and close this "shell mouth-hole" enabling it to feed.

During our research, observations and experiments were conducted on the exoskeleton plates on a plate-by-plate basis; that is, for each barnacle specimen, the exoskeleton was broken up into each of its plates, which were examined individually.

Materials & Methods

Live samples of Balanus Amphitrite were collected from Panacea, Florida, and kept in a saltwater tank until examination. Prior to examination, barnacle specimens were removed from the tank, dissected, and cleaned using tweezers, dental tools, and ethanol. The exoskeleton plates of one specimen were then separated (Figure 3, see appendix) and partially embedded in epoxy, using different orientations for each sample (i.e. right side up, upside down, and sideways). Sample Balanus amphitrite 2 (Ba2), however, was not broken up into individual exoskeleton plates, but rather left fully intact and embedded whole. Sample Ba2 was left complete in an attempt to image the plate-to-plate connections with the scanning electron microscope (SEM) (Figure 2), as well as to

determine whether there is any added mechanical strength due to the additional plates. All samples were subsequently polished flat with 600-grade sand paper, followed by nanometer alumina on a velvet pad to minimize visible nano-scale scratches. Prior to SEM experiments, the samples were carbon-coated to avoid electron charging during experiments. Samples were also dusted using a compressed-air duster to remove any microfibers that could distort SEM images.

Scanning Electron Microscopy (SEM) and Energy Dispersive X-ray Spectroscopy (EDS)

Scanning electron microscopy was used to image the micro-scale structure from samples of each orientation. The JEOL JSM636OLV was operated in high vacuum mode (hence the carbon-coating) and with zero stage-tilt. Images were taken using both the electron backscatter detector and the secondary electron detector, enabling information about atomic composition and topography to be collected. Energy Dispersive X-ray Spectroscopy (EDS) mapping of chemical and elemental components was done in select SEM images. It, too, operated in high vacuum, and chemical mapping was limited to C, O, Mg, Al, S, and Ca.

Nanoindentation

Two samples' hardness and elastic moduli were measured with Cornell University's TriboLab nanoindenter by Hysitron, Incorporated. The indenter measured hardness and elasticity by physically pushing on the sample with a nano-tip at a given force. The indenter gradually increased the load, held, and then released the load over a 15 second time interval, leaving an indent/impression in the sample. This impression consists of both permanent/plastic deformation and temporary/elastic deformation. The indenter then measured the size of the indentation, yielding an indentation load-depth hysteresis curve, providing hardness (H) and elastic modulus (Er). A more detailed explanation of the nanoindentation method can be found in [12], [23], [24].

Results

Data was collected from two B. Amphitrite (Ba) organisms. The exoskeleton of sample Ba1 was broken up into its 6 plates (labeled "a" through "f"1, as shown in Figure 3 (see appendix), each embedded with one of three orientations (top-up, bottom-up, side-up), while the exoskeleton of Ba2 was left intact and embedded top-up. SEM images were compiled to give a full view of each of the exoskeleton plate samples.

SEM images of Ba1c reveal a fine-grained dendritic structure, visible in Figure 5-c (see appendix). Note that the straight lines across the image are not structural, but rather are likely results of scratches from polishing or image searing due to electron-charging in the SEM. Figure 4 (see appendix) presents two more images revealing a similar dendritic pattern. Note the different orientation: Ba1c in Figure 5 is a side-up cross-section, whereas Ba1d and Ba2 in in Figure 4 are top-up cross-sections.

While there is structural information in the dendritic structure that these images reveal, the information that these images fail to explicitly illustrate is perhaps of equal value. We were not able to get clear images of the barnacle structure at magnifications

[1]Plates with outer attachments to both surrounding plates are labeled "a", while plates with inner attachments to both surrounding plates are labeled "b". All other plates in between are labeled "c" through "f".

greater than roughly 1500x due to a combination of sample and detector issues. Yet, even the highest magnification images do not display any organic components, nor do they expose much detailed structure beyond the dendritic structure visible in lower-magnified images. This means that the components we are looking for are far smaller than we were able to detect (likely on the order of nanometers). This in itself is a significant result because it provides a rough estimate of the size of the structural components within the barnacle exoskeleton.

To complement the structural information provided by SEM images, EDS data was taken on plate Ba1a (Figure 6 see appendix) to conduct chemical analysis. The plate was embedded in epoxy bottom-up (i.e. the base was polished off), giving a view of the barnacle from the bottom up. Figure 6-a shows two phenomena: the first is that the plate is actually formed by an inner-layer plate and an outer-layer plate that are attached together in a sort of zipper-like structure; and the second is there are holes visible as dark spots all along the plate. The holes are channels that run vertically up from the base of the exoskeleton to an undetermined point in the exoskeleton. Figure 6-b provides a detailed look at part of this zipper formation, while Figure 6-c, d gives us the chemical spectrum. The graph indicates high levels of calcium, carbon, and oxygen (which is to be expected as the shell is calcium carbonate-based), as well as some portion of magnesium and sulfur. The peak to the right of Ca is also calcium, just mapped at a different energy level.

In addition, nanoindentation was conducted on Ba1c and Ba2, each with four points in one area of the shell plate, to test the hardness and elastic modulus of the two plates (Table I, see appendix). The measured values of 59.05 ± 0.4 GPa and 2.9 ± 0.1 GPa for side-up and 68 ± 2.6 GPa and 3.1 ± 0.1 GPa for top-up fall within the range determined by previous studies on similar marine biomineral. Pérez-Huerta et al. (2008) conducted similar research on the shells of brachiopods, which are also calcite based, and found that the hardness and elastic modulus values fell within a range of approximately 2-5 GPa and 50-80 GPa, respectively. Both the averages and the individual indentation values from the barnacle sample fall within these ranges. This generally confirms that barnacle exoskeletons have relatively similar mechanical properties to brachiopod shells, though it does not necessarily provide evidence of congruent structures.

Of significant interest, the hardness and elastic modulus values collected from Ba1c and Ba2 show significant variation. This variation could be due to a number of variables: 1) The two samples were embedded with different orientations (90° to one another), 2) the indentations of the two samples were not necessarily taken in the same locations relative to edges, holes, plate-connections, etcetera, or 3) Ba2 had all six plates still attached to one another, whereas Ba1c was separated from all surrounding plates. From these experiments it is not possible to determine whether there is an asymmetry in the exoskeleton structure between different plate orientations that could be responsible for the variation observed in the hardness and elasticity or whether support from surrounding plates could affect the structural mechanics at the nanoscale level.

Conclusion

Balanus amphitrite has a complex dendritic microstructure that is visible in each plate regardless of orientation. The exoskeleton exhibits elemental components of calcium carbonate, and demonstrates mechanical properties similar to those of calcite

brachiopod shells. There is still significant research to be done. SEM images should be taken at much greater magnitude in effort to get detailed information about organic structural components, as well as more in-depth images of the micro-structural design itself. Additionally, more extensive nanoindentation data must be collected to determine the effect of variables: plate orientation, indent location on plate, detached plates vs. whole exoskeletons, organic components (conducted by baking samples, thereby extracting organics and leaving the mere calcite structure for testing), and the various elements found with EDS. Once greater hardness and elastic modulus data is available, samples should be re-analyzed with SEM in order to create detailed maps comparing hardness, elasticity, and elemental components for given regions of each plate. The combination of all this information will provide great insight into the mechanical strength observed in barnacle exoskeletons.

Acknowledgments

Nathan Swift would like to acknowledge Professor Rebecca Metzler and the Colgate University Physics Department for all their help and guidance throughout this research project. Additionally, he thanks lab technicians Richard Bomgardner, David Linsley and the Colgate University Geology Department for all their help with lab equipment and SEM use. Finally, he thanks Cornell University for the use of their nanoindenter

Bibliography

Addadi, L., Joester, D., Nudelman, F., & Weiner, S. (2006). Mollusk Shell Formation: A Source of New Concepts for Understanding Biomineralization Processes. *Chemistry European Journal , 12*, 980-987.

Barnes, H. (1956). Corrosion and shell composition in barnacles. *Nature* (177), 290.

Barthelat, F., Li, C.-M., Comi, C., & Espinosa, H. D. (2006). *J. Mater. Res. , 21* (8), 1977-1986.

Berman, A. (2008). Biomineralization of Calcium Carbonate. The Interplay with Biosubstrates. (A. Sigel, H. Sigel, & R. K. Sigel, Eds.) *Metal Ions in Life Sciences , 4*, 167-205.

Bourget, E. (1977). Shell structure in sessile barnacles. *Naturaliste , 104*, 281-323.

Bourget, E. (1987). Barnacle shells: Composition, structure, and growth. (A. J. Southward, Ed.) *Crustacean Issues* (5), 267-285.

Bütschli, O. (1908). Untersuchung über organische Kalkgebilde nebst Bermerkungen über organische kieselgebilde. *Abh. Ges. Wiss. Gottingen , 6*, 1-177.

Chave, K. E. (1954). Aspects of the biogeochemistry of magnesium. *J. Geol. , 620*, 266-283.

Clare, A. S., Ward, S. C., Rittschof, D., & Wilbur, K. M. (1994). Growth Increments of the Barnacle Balanus amphitrite Darwin (Cirripedia). *Journal of Crustacean Biology , 14* (1), 27-35.

Clarke, F. W., & Wheeler, W. C. (1922). The inorganic constituents of marine invertebrates. *prof. pap. I.S. Geol. survey , 124*, 1-62.

Currey, J. D. (1977). Mechanical properties of mother of pearl in tension. *Proceedings of the Royal Society of London Series B Biological Sciences , 196* (1125), 443-463.

Currey, J. D., Zioupos, P., Davies, P., & Casinos, A. (2001). Mechanical properties of nacre and highly mineralized bone. *Proceedings of the Royal Society of London Series B-Biological Sciences*, 268 (1462), 107-111.

Cusack, M., & Freer, A. (2008). Biomineralization: Elemental and Organic Influence in Carbonate Systems. Chemical Reviews , 108 (11), 4433-4454.

Janhunen, P., Toivanen, P. K., Polkko, J., Merikallio, S., Salminen, P., Haeggström, E., et al. (2010). Invited Article: Electric solar wind sail: Toward test missions. *Review of Scientific Instruments, 81* (111301), 1-11.

Kelly, A. (1900). über Conchit, eine neue Modifikation des kohlensauren Kalkes. *sb. bayer. Akad Wiss , 30*,187.

Lohse, D. P., & Raimondi, P. T. (2010). Barnacles. (M. W. Denny, & S. D. Gaines, Eds.) *Encyclopedia of Tidepools* , 61-64.

Lowenstam, H. A. (1964). Coexisting calcites and aragonites from skeletal carbonates of marine organisms and their strontium and magnesium contents. (Y. Miyake, & T. Koyama, Eds.) *Recent researches in the fields of hydrosphere, atmosphere, and nuclear geochemistry.* , 373-404.

Meigen, W. (1903). Beiträge zur Kenntnis des Kohlensäurenkalks. *Ber. naturf. Ges. , 13*, 1-55.

Newman, W. A. (1987). Evolution of Cirripedes and their major groups. *Crustacean Issues , 5*, 3-42.

Oliver, W. C., & Pharr, G. M. (1992). An improved technique for determining hardness and elastic modulus using load and displacement sensing indentation experiments. *Journal of Materials Research , 7*, 1564-1579.

Pérez-Huerta, A., Cusack, M., & Zhu, W. (2008). Assessment of crystallographic influence on material properties of calcite brachiopods. *Mineralogical Magazine , 72* (2), 563-568.

Sarikaya, M., & Aksay, I. A. (1992). Nacre of Abalone Shell: a Natural Multifunctional Nanolaminated Ceramic-Polymer Composite Material. (S. T. Case, W. Hennig, L. Nover, & U. Sheer, Eds.) *Results and Problems in Cell Differentiation , 19*, 1-26.

Sorby, H. (1879). Structure and origin of limestones. *Quart. J. Geol. Soc. Lond , 35*, 39.

Weiner, S., & Dove, P. M. (2003). An Overview of Biomineralization Processes and the Problem of the Vital Effect. (J. J. Rosso, P. M. Dove, J. J. DeYoreo, & S. Weiner, Eds.) *Reviews in Mineralogy and Geochemistry , 54*, 129.

Appendix

Figure 1

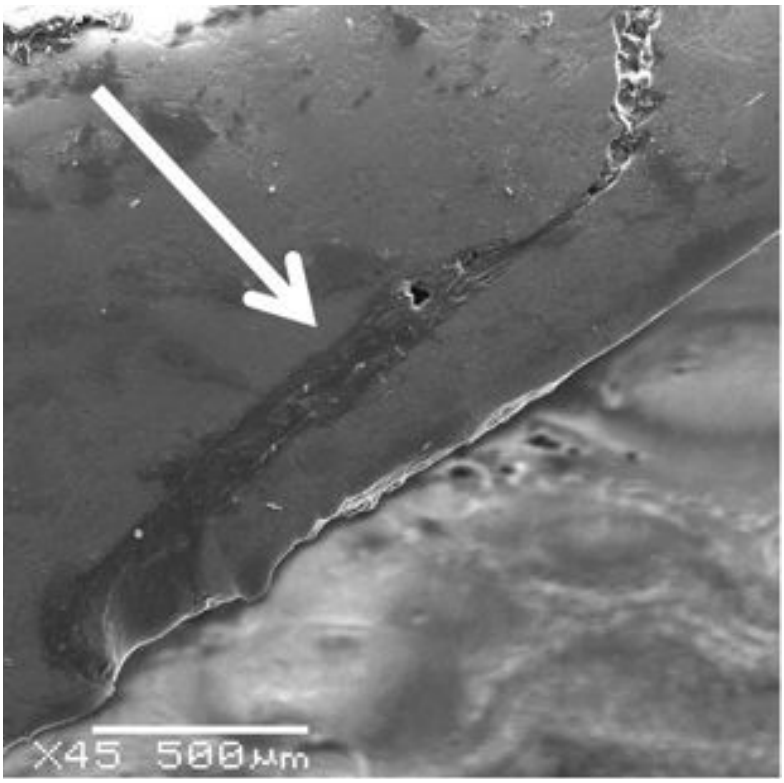

The layered connection between two exoskeleton plates on sample *Balanus amphitrite* 2 (Ba2).

Figure 2

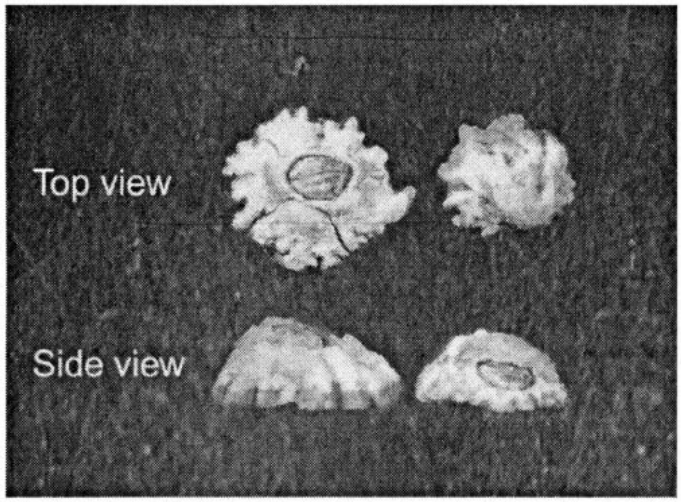

Top and side view of *Chthamalus anisopoma* showing the operculum in the center surrounded by test shells [17].

Figure 3

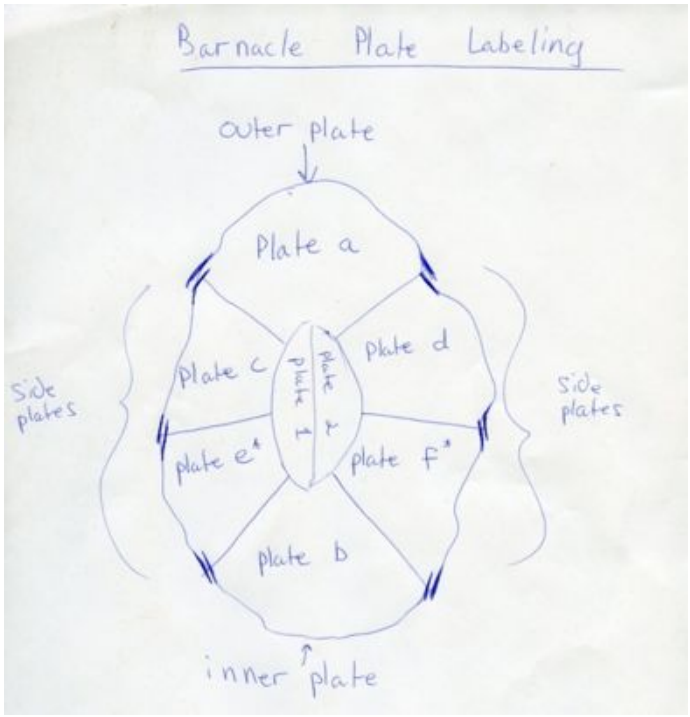

Exoskeleton plates labeled by their location on the organism and attachment to one-another.

* Because the amount of plates depends on species, not all plate labels continue beyond “d”.

Figure 4

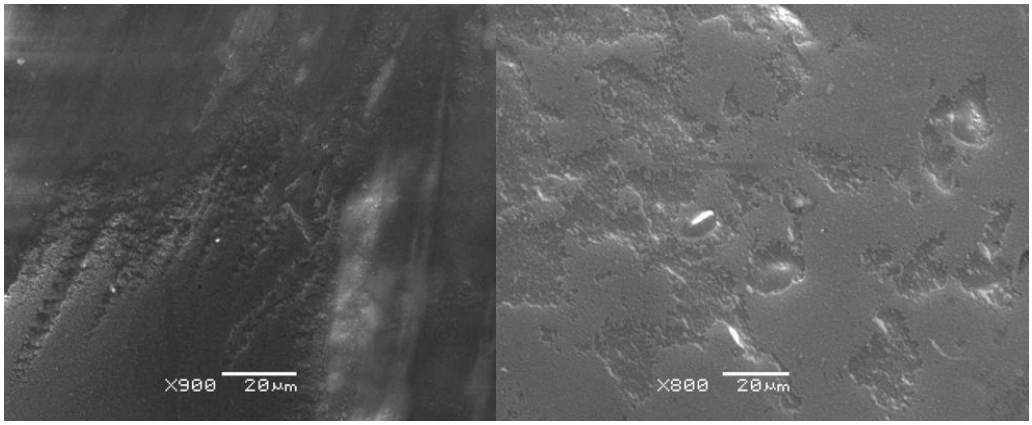

High magnification SEM secondary images of fine-grained dendritic structure on top-up sections of Ba1d (left) and Ba2 (right).

Figure 5

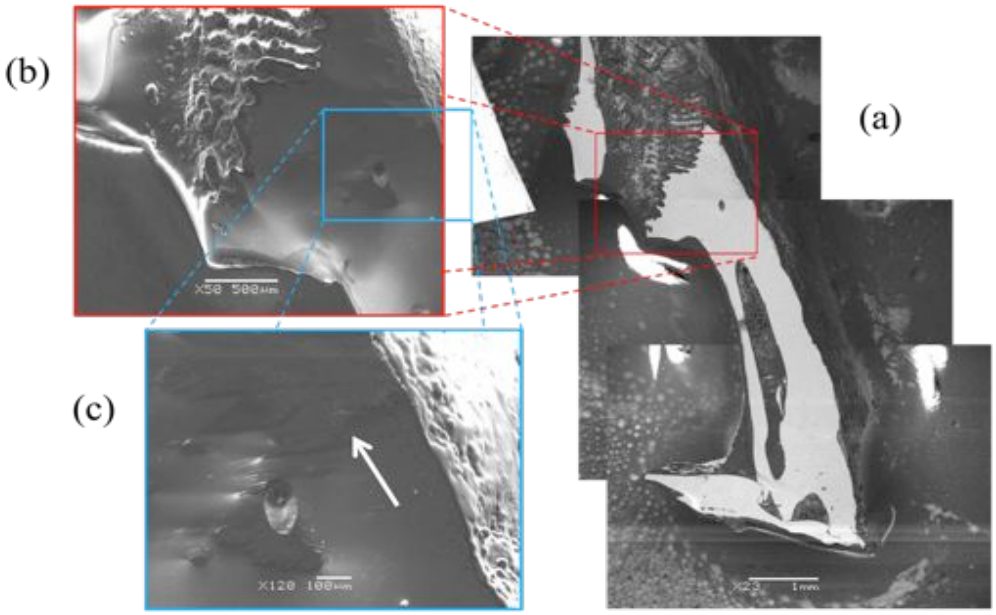

SEM images of the polished side-up section of plate Ba1c. (a) Compiled backscatter image of entire plate with holes and channels illustrated by dark regions; (b) higher magnification of an area of the plate with the secondary detector; (c) even greater magnification, showing visible dendritic structural lines toward the top (shown by arrow).

Figure 6

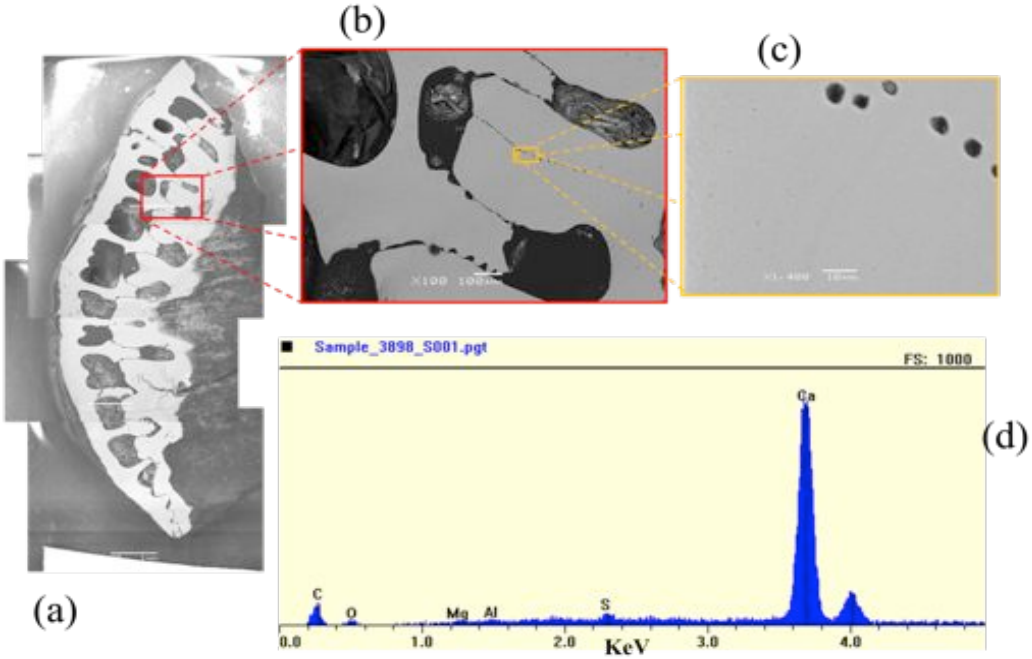

(a) Full SEM and EDS bottom-up section data on Ba1a; (b) increased magnification revealing 'zipper' structure; (c) even greater magnification image used for mapping EDS data; and (d) Ba1a EDS elemental data (with scale in keV).

Table 1

NANOINDENTATION DATA FOR ELASTICITY AND HARDNESS

	Ba1c -side Elasticity (GPa)	Ba2 - top Elasticity (GPa)	Ba1c - side Hardness (GPa)	Ba2 - top Hardness (GPa)
	61.54	65.80	2.91	3.08
	58.43	69.02	3.00	3.06
	62.07	69.44	2.76	3.03
	54.17	69.48	2.82	3.31
average	59.05	68.43	2.87	3.11
stdev	3.63	1.77	0.11	0.13
p-value	0.0040		0.014	

Values of hardness (H), elastic modulus (Er), and result statistics for plates Ba1c (side-up) and the intact exoskeleton of Ba2 (top-up).